ATRIAL SIGNALS 2021

KARLSRUHE, GERMANY

SEPTEMBER 23–25 2021

PROCEEDINGS

doi:10.5445/IR/1000138445

Städtisches Klinikum Karlsruhe

Karlsruher Institut für Technologie

Influence of Wave-Front and Atrial Tissue Properties on Eikonal Model Simulations

Cristian Barrios Espinosa[1], Nils Skupien[1], Guillaume Kachel[1,2], Olaf Dössel[1], and Axel Loewe[1]

[1]Institute of Biomedical Engineering, Karlsruhe Institute of Technology (KIT), Karlsruhe, Germany
[2]University of Clermont-Ferrand, Polytech, Aubière, France

Background

Atrial fibrillation (AF) is the most common arrhythmia in humans and current treatments are sub-optimal. Computational models have provided meaningful contributions in this field during the last years. However, the application of biophysically detailed models in the hospital is very challenging because their simulations are incompatible with regular procedure times. Eikonal models are significantly faster but less detailed. For example, they neglect the influence of wave-front (WF) and geomtrical tissue properties on conduction velocity (CV). Improvement of Eikonal models could contribute to better estimate AF risk.

Objective

To incorporate the influence of the geometrical properties of the electrical WF and atrial tissue on CV in Eikonal simulations.

Methods

The geometrical properties of the atrial tissue were set as suggested by Rossi et al. [1]. We conducted bidomain simulations in openCARP to calculate CV in meshes with different wall curvature and thickness. [2] The results were used to create a regression model which predicts CV when wall curvature and thickness are provided as inputs. Then, the predicted CVs were used as input for Eikonal simulations solved by the fast iterative method (FIM). Eikonal simulations and regression were performed in MATLAB.

Additionally, to incorporate the effects of WF properties, CV was obtained from bidomain experiments with different WF curvatures (WFC). A linear regression model was created to calculate CV based on WFC. The FIM was modified to calculate the propagation of the WFC and its influence on the CV.

Results

When including the geometrical properties of the atrial tissue, comparison between Eikonal simulations before and after the CV pre-processing shows a qualitative improvement, considering Rossi et al. as the reference. [1] In the experiments varying the WFC, there was a decrease of 55% of the mean error with respect to the bidomain simulations in the case with the highest curvature.

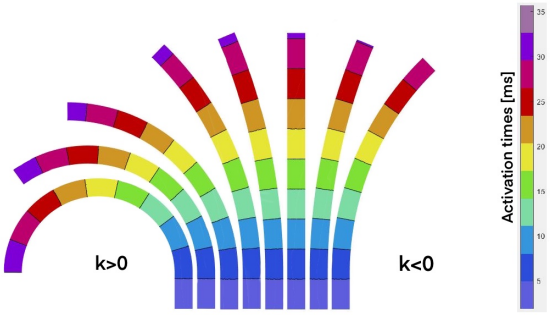

Figure 1: Eikonal simulations with different tissue curvatures.

Discussion

Changes in the Eikonal model provided more similar results to the bidomain simulations. This progress could lead to a better and faster risk assessment of patients with AF. However, further work is required to account for the combination of the studied effects in whole atria simulations.

References

[1] S. Rossi *et al.*, "Muscle thickness and curvature influence atrial conduction velocities," *Front Physiol*, vol. 9, p. 1344, 2018.

[2] G. Plank *et al.*, "The opencarp simulation environment for cardiac electrophysiology," *Comp Meth Progr Biomed*, p. 106223, 2021.

This project has received funding from the European Union's Horizon 2020 research and innovation programme under the Marie Skłodowska-Curie grant agreement No.860974.

Arrhythmogenicity of Genetic Mutations on a 3D Human Atrial Model

Rebecca Belletti[1], Lucia Romero[1], and Javier Saiz[1]

[1]Centro de Investigación e Innovación en Bioingeniería, Universitat Politècnica de València, Valencia, Spain

Background

Atrial fibrillation (AF) is the most frequent supraventricular arrhythmia and it has been related to the presence of genetic defects in genes encoding potassium channel protein structures in otherwise healthy patients. The arrhythmogenicity of three genetic mutations - KNCH2 T436M, KCNH2 T895M and KCNE3-V17M - has been previously studied at the cellular and tissue levels.

Objective

The aim of this study is to investigate the pro-arrhythmogenic effects of such mutations by modeling and simulating its electrical activities on a 3D atrial geometry.

Methods

The 3D hexahedral mesh, representing the human atrial model, is characterized by 21 regions and 56 subregions to account for heterogeneous histological properties and fiber orientation, and by a spatial resolution of 300 μm. The cellular electrical activity was modelled using a modified version of the Courtemanche-Ramirez-Nattel model, which includes both the formulation of the acetylcholine-activated potassium current and the parameters reproducing the genetic mutations' effects. Nine ionic models were implemented by tuning several ionic conductances to account for regional electrical properties. Longitudinal conductivities and anisotropy ratios were also tuned in each region to reproduce tissue heterogeneities and activation sequences. The electrical models were stabilized by applying 10 continuous beats to the sinoatrial node (SAN) with a 1000 ms basic cycle length (BCL). To get re-entrant activity, a train of 5 stimuli was applied to the coronary sinus (CS) region with a BCL of 160 ms for the mutation KCNH2 T436M, of 170 ms for KCNH2 T895M, and of 90 ms for the mutation KCNE3-V17M. During the CS pacing, the SAN was simultaneously stimulated by a 5-pulse train with BCL of 1000 ms. Temporal vulnerability to re-entrant activity for each mutation was computed as the width of the window when a train of stimuli in the CS would elicit a re-entry.

Results

The presence of the mutations increased the vulnerability of the atria to reentry and different types of arrhythmic behavior were observed. The KCNH2 T436M mutation presented a vulnerable window (VW) of 10 ms, and macro-reentries perpetuated for a minimum of 3.8 s and for a maximum of 5 s. In the presence of the mutation KCNH2 T895M, the VW has a 7 ms-width, and was characterized by the appearance of mostly macro-reentries and rotors, generated in the right atrium (RA) and perpetuating until the end of the simulations (5s). Finally, the VW for the KCNE3-V17M mutation was 24 ms-wide. In this case, all the rotors appeared in the CS area, moved around the RA walls and were sustained for the remaining simulation time. Collisions of multiple waves led to the formations of several instable rotors in both right and left atrium, wave breaks and to an overall more complex arrhythmogenic pattern.

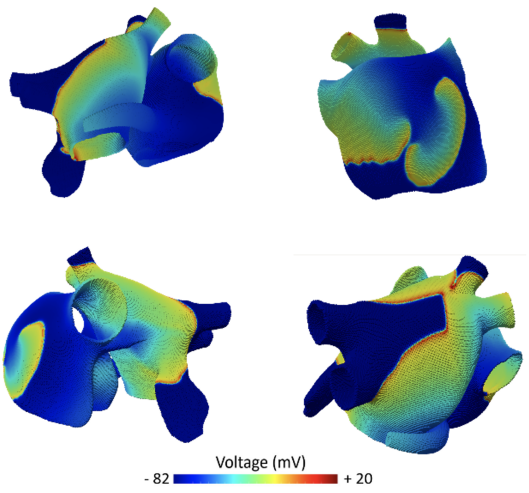

Figure 1: Simulation of complex spiral waves in 3D human atria in presence of the KCNE3-V17M mutation.

Discussion

This preliminary study supports that the presence of the genetic mutations in 3D human atrial model resulted in a more arrhythmogenic substrate, leading to mutation-dependent forms of arrhythmias.

Making More of Electrogram Morphology: Direction and Speed

D. Curtis Deno[1], Steven Kim[1], Patrick Kasi[1], Caleb Fick[1], Nicholas Ambrosius[1], Taras Rafa[1], Joe Rippke[1], Stéphane Massé[2], and Kumaraswamy Nanthakumar[2]

[1]Abbott Laboratories, Cardiac Electrophysiology, St. Paul, MN, USA
[2]University Health Network, Toronto General Hospital, Toronto, ON, Canada

Background

High density catheters with grid-like electrode arrangements enable more complete utilization of the information contained in electrograms. Recently, effort is being devoted to directly observing wavefront speed and direction. Omnipolar technology (OT) using electrogram morphology has recently been devised as an alternative method to conventional local activation timing (LAT) for instantaneously extracting speed and direction.

Objective

Determine the degree of agreement between OT and LAT methods of estimating local direction and speed from in vivo data.

Methods

Signals from identical 3-electrode cliques of Abbott's Advisor™ HD Grid Mapping Catheter Sensor Enabled™ were acquired from a pool of 10 maps and a total of 58,532 points in a variety of rhythms (SR, paced, AFL, AF) and chambers. Automated LAT determinations were made from unipolar dVdt timing whereas OT determinations were from unipole and bipole electrogram waveforms, ignoring activation timing. Clique signals were automatically scored for similarity to traveling waves (fixed shape, speed, direction) using OT Certainty, a machine learning derived index. Results are all mean ± standard deviation unless otherwise noted.

Results

In vivo, true directions and speeds are not known so accuracy could not be assessed. Wave directions were generally in agreement, correlated with R = 0.89 across all maps and points, rising to R = 0.97 when restricted to the 23% of points with OT Certainty > 0.7. A scatterplot of directions (not shown) revealed points clustered about the line of identity from 0-360°. Pooled angular discrepancies were often low, 0.6°±55.7° (median 0.0°, IQR 38.3°).

However, wave speed values across all maps and points were only modestly correlated, R = 0.34. Correlation improved to R = 0.41 with OT Certainty > 0.7. Pooled LAT speed was slightly less than OT speed (1.03±1.27 vs 1.15±0.74 m/s) though its variance was 3.0 times greater (1.61 vs 0.54 m^2/s^2, $p < 0.001$) as suggested in Figure 1.

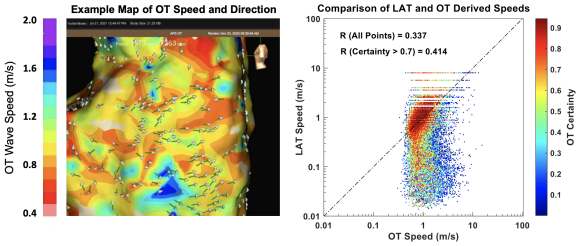

Figure 1: **Left**: Example map of OT speed and direction from a subject's RA during sinus rhythm. **Right**: Scatter plot of both LAT and OT speeds from all maps revealing widely distributed LAT speeds and greater agreement when OT Certainty was high.

Discussion

Mapping systems that display local direction and wave speed are under development and are hoped to contribute clarity to arrhythmia mechanisms and therapy options. This work compared two disparate approaches from 3 electrode cliques: LAT reflecting a detected instant and OT processing signals from a whole depolarization.

Both LAT and OT approaches produced plausible directions that were often in agreement. However, LAT derived speeds exhibited 3 times more variance than OT speeds. Wave speed 90th percentile values ranged from 0.10 to 3.84 m/s for LAT and 0.50 to 2.10 m/s for OT. This appeared to reflect LAT sensitivity to timing differences compared to OT which does not involve timing. Wave speed variation may also reflect challenges from ignoring transmural conduction and surface irregularity.

As high-density catheters evolve to shorter interelectrode spacings, increasingly local signals may better approximate traveling waves, favoring OT and becoming increasingly demanding of LAT. Both approaches may benefit from averaging over a larger number of electrodes, but at the expense of map resolution. Clinical requirements and benefits for accuracy and resolution from these new indices and grid-like catheters remain to be defined as a new era of mapping is beginning.

Correlation Between Rotors and Changes in Atrial Fibrillation Cycle Length in PersAF

Mahmoud Ehnesh[1], Xin Li[1,2,3], Tiago P. Almeida[1,2], Gavin S. Chu[2,3], Nawshin Dastagir[4], P.J. Stafford[2,3], G. André Ng[2,3], and Fernando S. Schlindwein[1,3]

[1]School of Engineering, University of Leicester, Leicester, UK
[2]Department of Cardiovascular Sciences, Glenfield Hospital, Leicester, UK
[3]National Institute for Health Research Leicester Cardiovascular Biomedical Research Centre, Leicester, UK
[4]University of Auckland, Auckland Bioengineering Institute, New Zealand

Background

Identifying ablation targets for persistent atrial fibrillation (PersAF) is still challenging despite attempts to guide ablation using Highest Dominant Frequency (HDF) and rotors.

Objective

The objective is to investigate the spatial correlation between rotor sites and sites of Atrial Fibrillation Cycle Length (AFCL) changes that lead to AF termination in PersAF.

Methods

Ten patients underwent a first time HDF-target PersAF ablation in the left atrium (LA). LA was mapped using non-contact array (Ensite, Abbott / St. Jude Medical). Virtual electrograms (VEGMs) from 2048-channels (30 s duration) were exported into MATLAB and QRST-subtraction was performed, then target HDF sites were identified and ablated. LA AFCL was measured pre- and post-ablation of each of the HDF sites. The pre- and post-ablation rotors sites and sites of AFCL changes during ablation were compared using spatial correlation, for terminated and non-terminated patients.

Results

AF was terminated in 40% of enrolled patients. Although the results suggest poor spatial correlation between rotors sites and sites of AFCL changes in terminated and non-terminated patients, higher correlation was found in terminated patients (spatial overlapping percentage 25±4.2% Vs. 11±3.7%, respectively). Additionally, global HDF decreased for terminated patients (pre: 9.4±1.1 Hz Vs. post: 8.2±0.4 Hz, $P < 0.001$) and increased in non-terminated patients (pre: 7.8±1.7 Hz Vs. post: 9.3±0.8 Hz). In terminated patients, LA ablation reduced the number of rotors (pre- Vs. post-ablation, 19±7.8 Vs. 4.2±0.2), rotor lifespan (9.6±0.09 ms Vs. 8.7±0.1 ms, $P<0.001$), rotor displacement (3.3±1.3 mm Vs. 2.3±1.3 mm) and rotor velocity (2.8±0.9 mm/ms Vs. 1.4±0.8 mm/ms). Conversely, LA ablation increased the number of rotors (pre- Vs. post-ablation, 11±3.8 Vs. 22±8.2), rotor lifespan (7.7±0.11 ms Vs 8.4±0.1 ms, $P<0.001$) and rotor velocity (0.9±0.7 mm/ms Vs. 1.3±0.5 mm/ms) in non-terminated patients, and reduced rotor displacement (3.5±1.4 mm Vs. 2.3±0.6 mm).

Discussion

Our results have shown that using 30 s noncontact VEGMs rotors sites demonstrated poor simultaneous spatial overlapping of the location of rotors and sites of AFCL changes that lead to AF termination suggesting that, if there is interaction between these 2 proxies of PersAF, the dynamics of such interaction is more complex than a simple simultaneous spatial correlation. The number of rotors and rotors' parameters did change following HDF-target ablation in terminated patients.

Cellular Variability within the In-Silico Atria and its Impacts on Conduction Velocity in Healthy and AF Remodeled Tissue

Jordan Elliott[1], Maria Kristina Belen[1], Luca Mainardi[2], Valentina Corino[2], and Josè Felix Rodriguez Matas[1]

[1]Department of Chemical and Material Engineering, Politecnico Di Milano, Milan, Italy, 20133
[2]Department of Electronic, Information and Bioengineering, Politecnico Di Milano, Milan, Italy, 20133

Background

Atrial models are increasingly relied upon to understand the mechanisms behind atrial arrhythmias such as atrial fibrillation. In order to represent the behaviour of the atria, it is important to create representative models of the human atria. Due to difficulties incorporating cellular variability, models typically assume cellular coupling masks the impact of electrophysiological variability on the cellular level. Electrophysiological models typically only vary at a regional level. Recent studies have shown that cellular variability may have a larger impact on electrophysiological behaviour than previously expected.

Objective

The objective of the study is to determine the impact of cellular variability on the propagation across isolated tissue and whole atrial models for both healthy and AF remodeled tissue. This is completed through observing the impact on conduction velocity and the atrial depolarization and repolarization.

Methods

A population of unique cellular models was created using the Courtemanche cellular model. Published experimental data was used to divide the population into 8 regional populations based on 5 biomarkers (RMP, APA, APD20, APD50, APD90). Regionally homogenous and heterogeneous tissue samples were separately calibrated to target experimental CV values. The variability in CV across 10 heterogeneous models were compared for each atrial region. Activation maps and APD maps were calculated for whole atria simulations of the regionally homogenous and heterogeneous models.

Results

Isolated heterogeneous tissue results using the same tissue conductance showed the standard deviation in CV ranged from 0.19cm/s to 2.4cm/s depending on atrial region. Similar variability in CV was observed between healthy and AF remodelled tissue samples. Figure 1 shows the regional variability in CV across the 10 heterogeneous models. In the healthy atria, whole atrial simulations showed heterogeneous models resulted in a similar average total activation times (TAT) compared with the regionally homogenous model (117ms), varying between 117ms and 118ms. Depolarization across the regionally homogenous model and the variable models remained consistent for both the healthy and AF remodelled atria. Repolarization in the variable atrial models was faster than in the homogenous model.

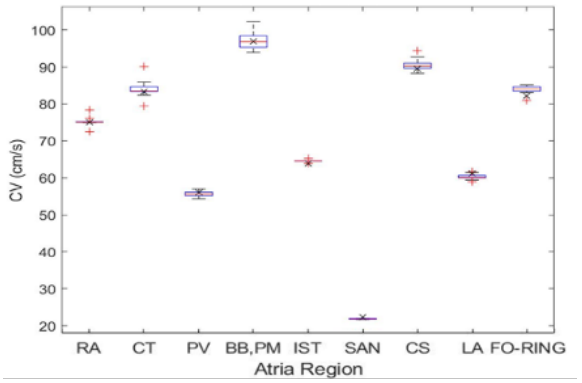

Figure 1: Boxplot showing variability in CV across AF remodeled atrial regions due to cellular variability.

Discussion

Cellular variability across isolated tissue results in CV variation of up to 4cm/s. Unsurprisingly, electrophysiological variability has a negligible impact on depolarization across the atria. Most of the observed variability in activation times is caused by anatomical variability. Electrophysiological variability results in an earlier and faster repolarization phase for both the healthy and AF remodelled atria. This could have a significant impact on the susceptibility to the maintenance of AF episodes. Accounting for cellular variability could result in models better representing healthy atrial behaviour and that of different arrhythmias.

Left Atrium Hemodynamic in Atrial Fibrillation and Normal Subjects

Matteo Falanga[1], Alessandro Masci[1], Antonio Chiaravalloti[2], Fabio Ansaloni[2], Corrado Tomasi[2], and Cristiana Corsi[1]

[1]DEI, University of Bologna, Campus of Cesena, Bologna, Italy
[2]Santa Maria delle Croci Hospital, AUSL della Romagna, Ravenna, Italy

Background

A computational fluid-dynamics (CFD) model previously developed with the aim of evaluating cardioembolic risk in patient affected by atrial fibrillation (AF) was used for the characterization of the left atrium (LA) hemodynamic in normal subjects (NL), patients affected by paroxysmal atrial fibrillation (PAR-AF) and patients affected by persistent atrial fibrillation (PER-AF).

Objective

Based on the fluid-dynamics simulations results, we aimed at enhancing differences in blood flow in AF patients and NL and at better understanding the relationship between AF progression and stroke risk on a patient-specific basis.

Methods

3D patient-specific anatomical and motion models were derived from ECG-gated coronary artery CTs acquired with retrospective protocol. These models represented the computational domain for CFD simulations in which inflow initial conditions were derived from PW Doppler at the mitral valve and at the pulmonary veins. Velocity field and vortex structures both within the LA and left atrial appendage (LAA) were assessed in 10 NL, 5 PAR-AF and 4 PER-AF. Blood stasis was evaluated by populating the LAA with 500 particles and counting the number of particles still present after five cardiac cycles.

Results

Velocities inside the LA and in the LAA presented different amplitude and distribution in the 3 groups (peak velocity – NL: 50÷60 cm/s, PAR-AF: 40÷50 cm/s, PER-AF: 15÷25 cm/s). The mean velocity resulted lower in the PAR-AF compared with PERS-AF (mean velocity – PAR-AF: 25÷35 cm/s, PER-AF: 8÷20 cm/s) at the LAA ostium and inside the LAA, in which the washout effect was strongly reduced (Figure 1). On the other hand, the mean velocity in the NL was higher with respect of AF patients (mean velocity – NL: 40÷45 cm/s). A higher number of vortex structures was observed in NL compared with AF patients, thus favoring the hypothesis of a more efficient wash-out of the LA and of the LAA. The fluid particle analysis in the LAA confirmed these results (NL: 5±2, PAR-AF: 18±3, PER-AF: 41±10).

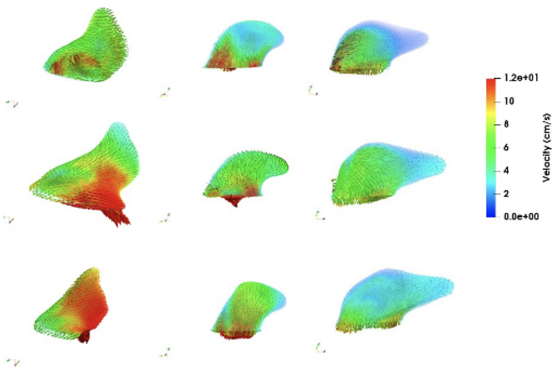

Figure 1: LAA velocity fields in 3 representative subjects (NL, PAR-AF and PER-AF in the 1st, 2nd and 3rd column respectively), in three phases of the cardiac cycle (1st row: ventricular systole, 2nd row: ventricular diastole, 3rd row: atrial systole).

Discussion

Velocities within the LA and LAA showed higher values in the NL subjects with respect to PAR-AF and PER-AF patients. The lowest values within the LA and LAA were observed in the PER-AF group that could imply a higher probability of blood stasis and consequently an increase of stroke risk. In PAR-AF patients the contractility was not strongly reduced as for the PER-AF patients thus leading to higher values of the velocities and a stronger LA contraction/expansion with respect to the PER-AF. This may reduce the probability of clot formation. In addition, vortex structures, LAA ostium velocity, and the LAA residence time analysis confirmed what we qualitatively expected about the differences of the three groups. The developed approach quantifies differences in LA hemodynamic between AF and NL patients, also allowing a stratification of the disease progression in terms of variations in the blood velocity, organization of blood flow and quantification of blood stasis.

An Evaluation on the Clinical Outcome Prediction of Rotor Detection in Non-Invasive Phase Maps

Carlos Fambuena-Santos[1], Ismael Hernández-Romero[1], Rubén Molero[1], Andreu Martínez Climent[1], and María del la Salud Guillem Sánchez[1]

[1]ITACA Institute, Universitat Politècnica de València, Valencia, Spain

Background

Electrocardiographic imaging (ECGI) and phase maps have been used in the past for rotor identification and ablation guidance in atrial fibrillation (AF).

Objective

This study proposes a new rotor detection algorithm based on phase singularities (PSs) detection in phase maps. It also evaluates the potential of rotor-related metrics for clinical outcome prediction in patients undergoing pulmonary vein isolation (PVI).

Methods

The performance of the new algorithm was evaluated using real AF episodes. Visually identified rotors were manually labelled using a custom application. Phase maps reconstructed from ECGI signals in 29 patients were calculated prior PVI with and without adenosine injection. Different rotor metrics were calculated and compared between patients that recovered from PVI and patients that persisted in arrhythmia 6 months after ablation. These parameters were calculated using 2 different implementations of the algorithm. In the first one the PSs that did not belong to rotors spinning for at least 1 turn (short lasting rotors) were filtered, and in the second one no filtering was applied to the PS.

Results

The mean precision and recall values of the algorithm were 0.83 and 0.85. A significantly higher concentration of phase singularities was found in the PPVV in patients that recovered from PVI (12.06 vs 6.49%, $p < 0.01$ using adenosine and filtering of 1 turn). In contrast, the number of rotors per second in the atria was higher in patients that did not recover from PVI (66.81 vs 51.13, $p < 0.05$ using adenosine and no turn filtering).

Discussion

The use of adenosine and turn filtering affect the distributions of PSs found in the different atrial regions as well as the number of rotors detected.

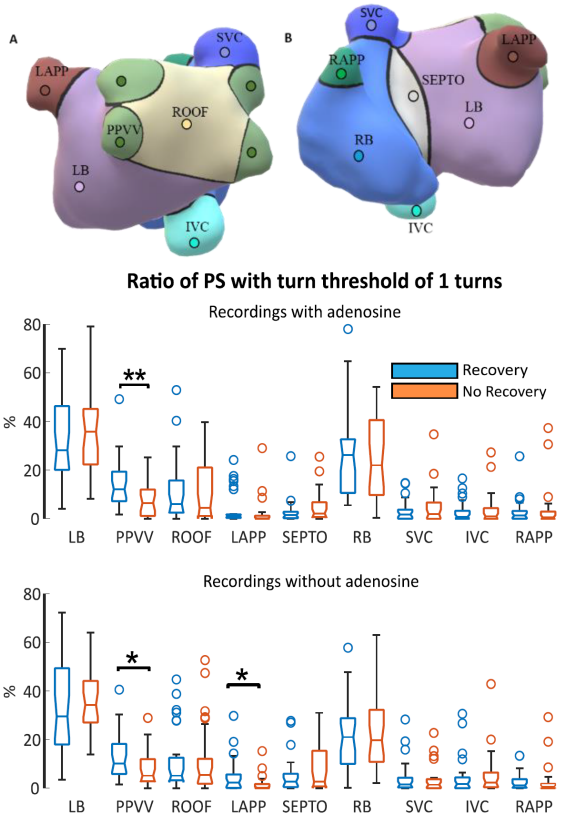

Figure 1: A & B) Front and back view of the atrial model and regional subdivision employed in the analysis. C) Proportion of PSs found in all the defined atrial regions in patients that recovered from PVI (Recovery group) and patients that return to arrythmia (No recovery).

Adenosine seems to reduce the number of regions with a statistically significant difference in the proportion of PS. Furthermore, an increase in the significance of this difference was found in the PPVV when adenosine and turn filtering were combined.

The difference found in the number of rotors between the studied groups became more significance when no adenosine was used and no filtering was applied. The results obtained in this study suggest that rotor-related metrics calculated from phase maps contain relevant information to predict clinical outcome in PVI patients.

Spatial Distribution of Repetitive Electrograms Identifies a Spectrum of Organization from Atrial Fibrillation to Flutter

Prasanth Ganesan[1], Miguel Rodrigo[2], Brototo Deb[1], Ruibin Feng[1], Neal K Bhatia[3], Albert J Rogers[1], Paul Clopton[1], Wouter-Jan Rappel[4], and Sanjiv M Narayan[1]

[1]Stanford University Department of Cardiovascular Medicine, Palo Alto, CA, USA
[2]Universitat de València, Spain [3]Emory School of Medicine, Atlanta, GA, USA
[4]University of San Diego, La Jolla, CA, USA

Background

Atrial fibrillation (AF) may show regional organization in the frequency domain, in vectors, and in potential drivers, but tools used to map organization in AF are clinically non-intuitive and have low reproducibility between centers.

Objective

To test the hypothesis that a novel method to identify regions within which spatial electrogram (EGM) patterns repeat with a high correlation may serve as an effective tool for decoding organization in AF.

Methods

REpetitive ACTivity (REACT) mapping computes spatiotemporal correlation of unipolar electrograms (EGMs) at all 2x2 spatial grids from a 64 pole Basket catheter (Figure A). A REACT value indicates the *degree of repetition* (range: 0 to 1, 1=highest repetition) of activation timing and morphology (shape) within the recording window.

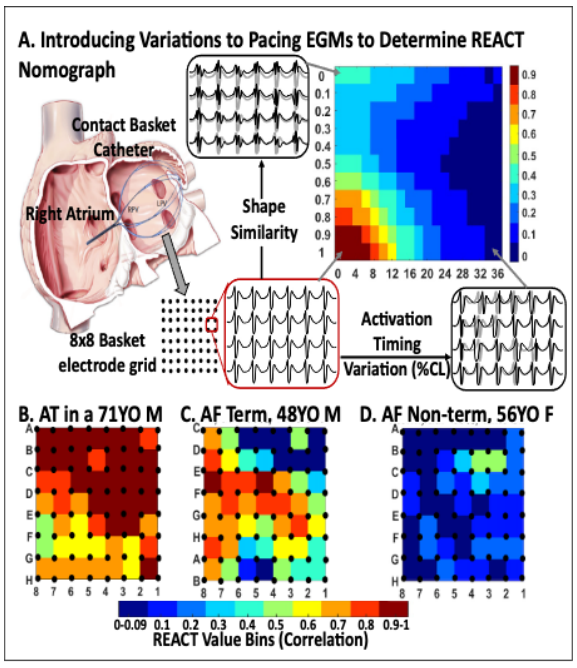

We systematically evaluated our algorithm to assess: (i) Function Nomograph: We introduced stochastic variations in activation timing (% cycle length) and shape (similarity to original shape) of EGMs recorded during clinical pacing (highly repetitive EGMs) to simulate decreasing levels of repetition (Figure A). We then applied REACT mapping on each of these simulated signals to determine the nomograph of REACT. We averaged the nomograph for N=100 trials of random values. (ii) Clinical significance: We recruited N=70 patients (age 63.0±10.1yrs, 67.6% male) in groups (I) N=10 patients with AT, (II) N=30 patients with AF that terminated by ablation, and (III) N=30 AF patients without termination. We applied REACT mapping offline to 4sec EGMs, and assessed the spatial distribution of repeating EGM islands in each of the 3 groups.

Results

Nomograph of REACT (Figure A) indicates highest value for pacing EGMs with minimal variations, which monotonically decreased for rhythms with increasing variation. For similarity<0.4, there were fewer unique signals. The calibrated nomogram was used to interpret the extent of variability present in our arrhythmia cases. Fig B-D illustrate patient examples from each group with islands of repeating EGMs (≥0.5 REACT). (B) In AT, the entire atrium shows high REACT scores (100%); (C) In AF that terminated, a spatial zone of high REACT values were present (67.4% of mapping field); (D) In AF that did not terminate by ablation there was little organization, with repeating EGM islands occupying only 4.1% of the atrium. Overall, areas of repetitive EGMs indicated a hierarchy of organization from patients with (I) AT (80.7±16.3% mapped field), to (II) AF that terminated (56.4±28.3%) then (III) AF that did not terminate (25.9±21.3, p<0.001).

Discussion

REACT is an intuitively plausible tool to quantify organization in human AF and AT. Future studies could use REACT to identify patients who may benefit most from ablation, and to gain mechanistic insights into AF phenotypes.

Influence of the Right Atrium for Arrhythmia Vulnerability: Geometry Inference Using a Statistical Shape Model

Patricia Martínez Díaz[1], Luca Azzolin[1], Jorge P. Sánchez Arciniégas[1], Claudia Nagel[1], Olaf Dössel[1], and Axel Loewe[1]

[1]Karlsruhe Institute of Technology, Institute of Biomedical Engineering, Karlsruhe, Germany

Background

Personalized computer models incorporate clinical data to simulate arrhythmia mechanisms in a patient-specific manner with the potential to guide therapy planning. The geometry can be obtained from magnetic resonance images (MRI) and other imaging techniques as well as from electro-anatomical mapping system (EAMS). However, the availability of clinical data can be limited and, in some cases, only information from the left atrium (LA) is available. Such single chamber models would neglect the influence of the right atrium (RA) on the initiation and maintenance of the arrhythmia. In this context, statistical shape models (SSM) can be a way to infer a bi-atrial geometry when only mono-atrial data are available.

Objective

Compare the differences in arrhythmia vulnerability under 4 different LA and RA combinations: A) Bi-atrial geometry from MRI, B) Bi-atrial model where both LA and RA were used to fit the SSM, C) Bi-atrial model where only the LA was used to fit the SSM, D) Mono-atrial LA model from MRI.

Methods

Data were collected from 6 healthy volunteers and 2 AF patients. For each patient, the bi-atrial MRI model was defined as the reference scenario (A). First, the bi-atrial MRI geometry was used to fit a bi-atrial SSM (B) [1]. Then, an additional bi-atrial model was generated (C) in which the RA geometry was inferred from the population-level statistical distribution based purely on patient-specific LA information. The last case (D) was composed of just LA MRI data. Fiber orientation and anatomical regions were annotated [2] and the Pacing at the End of the Effective Refractory Period (PEERP) protocol [3] was used to test arrhythmia inducibility in all model variants by pacing from a set of evenly distributed points covering the epicardial surface. To simulate monodomain simulations conducted with openCARP [4]. Finally, the number of inducing points, the complexity of the arrhythmia and the areas prone to maintain micro-reentries were compared between the four geometrical instances.

Discussion

When assessing vulnerability in a LA-only model, some rotors may not be sustained due the reduced area. Therefore, we inferred the RA and generated a bi-atrial model to overcome this limitation. This approach could be considered as well when only LA-EAMS data are available.

References

[1] C. Nagel *et al.*, "A bi-atrial statistical shape model and 100 volumetric anatomical models of the atria," *Zenodo*, 2020.

[2] R. Piersanti *et al.*, "Modeling cardiac muscle fibers in ventricular and atrial electrophysiology simulations," *Computer Methods in Applied Mechanics and Engineering*, vol. 373, p. 113468, 2021.

[3] L. Azzolin *et al.*, "A reproducible protocol to assess arrhythmia vulnerability : Pacing at the end of the effective refractory period.," *Frontiers in Physiology*, vol. 12, p. 656411, 2021.

[4] G. Plank *et al.*, "The openCARP simulation environment for cardiac electrophysiology," *Computer Methods and Programs in Biomedicine*, vol. 208, p. 106223, 2021.

Acknowledgement

This Project has received funding from the European Union's Horizon research and Innovation programme under the Marie Skłodowska-Curie grant agreement No. 860974.

Analyzing the Effect of Catheter-Sheath Overlapping Status in Local Impedance Simulations

Carmen Martínez Antón[1], Laura Anna Unger[1], and Olaf Dössel[1]

[1]Karlsruhe Institute of Technology, Institute of Biomedical Engineering, Karlsruhe, Germany

Background

In the heart, areas of scar and different levels of fibrotic tissue have been identified as potential driving regions of arrhythmic activity. These areas are typically characterized by magnetic resonance imaging or low voltage maps. Since both the aforementioned modalities entail drawbacks when concluding on the underlying substrate, local impedance (LI) measurements have gained attention recently. Intracavitary LI recordings can provide the information required to locate regions of pathologically altered substrate as changes in conductivity may indicate alterations in myocardial functionality. In this context, identifying the factors contributing to the measured LI is a matter of importance to provide accurate and reliable assessments. However, in clinical practice physicians face artifacts that flaw LI values, such as the overlap between segments of the catheter and the steerable sheath.

Objective

To identify the effect of different overlapping status between a steerable sheath and catheter segments in LI measurements by means of in silico experiments.

Methods

Precise, three-dimensional models [1] of the catheters IntellaNav MiFi™ OI and IntellaNav StablePoint™ (Boston Scientific, Marlborough, MA, USA) were developed.

A steerable sheath was added varying its relative position to the ablation catheter to change the degree of overlap between both elements were embedded into a blood box. Meshes were generated to simulate different combinations of catheter-sheath overlapping status with GMSH 4.4.1. and a simulation environment predestined for impedance studies. Distinct conductivities were assigned to electrodes, insulators, and the surrounding blood. Knowing the injected current between the tip and the proximal ring electrode, the simulation can be defined as a forward problem with a unique solution. Clinical studies and in vitro experiments were performed at the Städtisches Klinikum Karlsruhe to validate the simulation results with real sheath artifact problems.

Results

A simulated trace of LI values while moving the sheath along the catheter is shown in Fig. 1. As it was reported in clinical studies, LI measurements increase significantly when reaching the proximal ring.

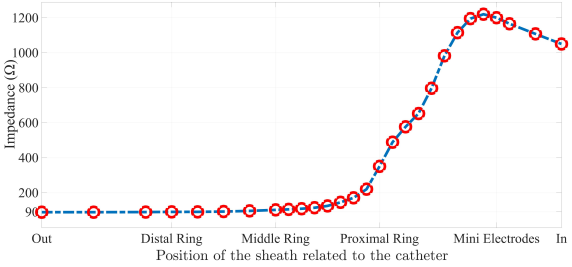

Figure 1: LI values simulated trace as the distal segment of the sheath overlaps the catheter IntellaNav MiFi™ OI.

Discussion

During an electrophysiological study, a steerable sheath is required to help with catheter stability and navigation. However, if the sheath overlaps with one or more of the electrodes, a significant distortion occurs in the LI measurement. Computational models help to understand and solve this artifact, particularly in the boundary regions with marginal but clinically significant LI alterations.

References

[1] S. Pollnow *et al.*, "Mini electrodes on ablation catheters: Valuable addition or redundant information? insights from a computational study," *Computational and Mathematical Methods in Medicine*, 2017.

Acknowledgement

This Project has received funding from the European Union's Horizon research and Innovation programme under the Marie Skłodowska-Curie grant agreement No. 860974.

A Numerical Study of Atrial Fibrillation Electrophysiological Substrate based on High-Density Mapping

Stefano Pagani[1], Antonio Frontera[2], Luca Dede'[1], Luca R. Limite[2], Matteo Salvador[1], Andrea Manzoni[1], Paolo Della Bella[2], and Alfio Quarteroni[1,3]

[1]Politecnico di Milano, MOX-Department of Mathematics, Milan, Italy
[2]I.R.C.C.S. San Raffaele Hospital, Arrhythmology and Electrophysiology Unit, Milan, Italy
[3]École Polytechnique Fédérale de Lausanne, Institute of Mathematics, Lausanne, Switzerland

Background

Catheter ablation guided by high-density electroanatomical (EA) maps constitutes an established procedure for managing atrial fibrillation (AF). Electrogram signals collected in sinus rhythm allow the reconstruction of the electrical wavefront propagation and the localization of electrical abnormalities. However, the interpretation of EA maps and the consequent definition of ablation strategies in the different forms of AF are subject to continuous debate.

Objective

This study aimed to quantitatively characterize the electrophysiological substrate of patients suffering from paroxysmal and persistent AF using numerical simulations parametrized with EA activation maps acquired during sinus rhythm.

Methods

We constructed a computational pipeline to simulate the formation and sustainment of localized reentrant circuits in patients affected by paroxysmal and persistent AF. We first processed the EA activation maps by computing conduction velocities with a least-square approach, providing a quantitative characterization of the main electrophysiological properties (slow conduction corridors, wavefront collisions, and pivot points). Conduction velocities were then adopted to parametrize a coupled model for cardiac electrophysiology formed by the monodomain equation and a system of ordinary differential equations describing the ionic species dynamics. This parametrization provided a detailed characterization of the heterogeneous electrical and structural properties responsible for different reentry mechanisms. Finally, we numerically predicted with the parametrized model the dynamics of localized reentrant circuits by simulating ectopic beats originating from the pulmonary veins.

Results

The numerical results highlighted the role of conduction properties' distribution in the formation and sustainment of different localized reentries. Specifically, heterogeneous areas led to head-tail interactions, which generated unstable localized reentries with moving rotors. Instead, areas with severe slow conduction corridors led to the anchoring of the rotors and, consequently, to the sustaining of the phenomenon.

Discussion

The quantitative analysis of the electrophysiological substrate showed a progression in the number and the severity of slow conduction corridors moving from paroxysmal to persistent AF. Numerical simulations associated the latter form of AF with an augmented probability of localized reentries anchoring in severe slow conducting areas. On the contrary, the less frequency of these areas, together with head-tail interactions, determined unstable localized reentries in the paroxysmal case.

Acknowledgements

This project has received funding from the European Research Council (ERC) under the European Union's Horizon 2020 research and innovation programme (grant agreement N. 740132).

Analysis of Unipolar Electrogram Eigenvalue Dispersion for the Detection of Atrial Fibrosis

Jennifer Riccio[1], Alejandro Alcaine[2,1,3], Sara Rocher[4], Javier Saiz[4], Juan Pablo Martínez[1,3], and Pablo Laguna[1,3]

[1]BSICoS, I3A, IIS Aragón, Universidad de Zaragoza, Zaragoza, Spain
[2]Facultad de Ciencias de la Salud, Universidad San Jorge, Zaragoza, Spain
[3]CIBER en Bioingeniería, Biomateriales y Nanomedicina (CIBER-BBN), Spain
[4]Ci2B, Universitat Politècnica de València, Valencia, Spain

Background

Atrial fibrosis plays a meaningful role in the pathogenesis of atrial fibrillation (AF). Areas with peak-to-peak amplitude of bipolar electrograms (b-EGMs) lower than 0.5 mV are detected as scar tissue and targeted for AF ablation procedures. However, this approach disregards the spatiotemporal information held in the signal and is influenced by b-EGMs dependence on catheter orientation.

Objective

To overcome these limitations, in this study, we propose to use the dominant-to-remaining eigenvalue dominance ratio (EIGDR) of unipolar electrograms (u-EGMs) within a group of nearby electrodes (clique) as a measure of the voltage wavefront roughness and correlate it with the presence of fibrosis.

Methods

We simulated u-EGMs from a 2D atrial tissue, including a circular patch of diffuse fibrosis, following the Courtemanche model. They were corrupted with one hundred different realizations of real noise with level $\sigma_n = 33\ \mu V$. One hundred different maps of three EIGDRs ($\mathcal{R}$: ratio of first eigenvalue of u-EGMs correlation matrix to the sum of all the others; $\mathcal{R}^{\mathcal{A}}$: same ratio after u-EGMs time alignment within the clique; and $\Delta\mathcal{R}^{\mathcal{A}}$: the gain in eigenvalue concentration produced by alignment) were obtained using two clique sizes (3×3 and 2×2) and three catheter orientations (0°, 30° and 45°). The maximum accuracy for fibrosis detection (ACC) was used as performance measurement. The threshold for maximum accuracy was obtained jointly for the three orientations, assuming that the angle between the propagation direction and the catheter is not known a priori. For performance comparison, maps of peak-to-peak voltage of b-EGMs in each of the two catheter directions (V^{b-x} and V^{b-y}) and of their maximum (V^{b-m}) were also tested.

Results

The proposed EIGDR indices show the following average performance (mean ± standard deviation): ACC = 0.84 ± 0.01, 0.88 ± 0.01 and 0.80 ± 0.02 for $\mathcal{R}$, $\mathcal{R}^{\mathcal{A}}$ and $\Delta\mathcal{R}^{\mathcal{A}}$, respectively, when 2×2 cliques are used. With the 3×3 configuration, ACC = 0.87 ± 0.02, 0.95 ± 0.02 and 0.88 ± 0.02 for the same indices. Bipolar voltage maps achieve ACC = 0.69 ± 0, 0.86 ± 0.01 and 0.91 ± 0.01, for V^{b-x}, V^{b-y} and V^{b-m}, respectively.

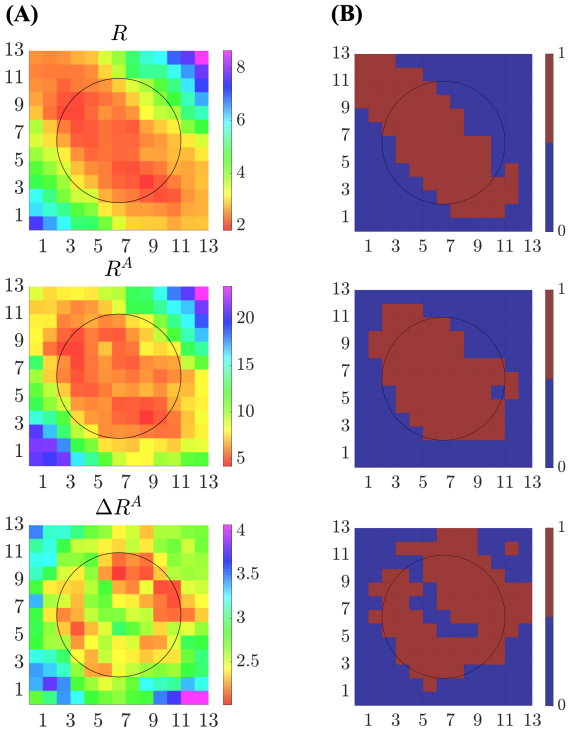

Figure 1: **(A)**: EIGDR maps for 3×3 cliques and 45° catheter for one noise realization. **(B)**: identification masks for ACC thresholds.

Discussion

EIGDR approach allows to discriminate fibrotic from non-fibrotic tissue, improving its performance when clique alignment is considered and 3×3 configuration is used, providing slightly improved performance to standard voltage maps for the 3×3 aligned EIGDR maps.

Effect of Extra Lesions on AF burden of Continuously Monitored Patients Undergoing Single-Procedure Catheter Ablation

Javier Saiz-Vivo[1], Valentina D.A. Corino[2], Mirko de Melis[3], and Luca T. Mainardi[2]

[1]Medtronic: Bakken Research Center, Maastricht, Netherlands
[2]Department of Electronics, Information and Bioengineering, Politecnico di Milano, Milan, Italy

Background

Catheter Ablation (CA), specifically pulmonary vein isolation (PVI) is a well stablished procedure for patients suffering from Atrial Fibrillation (AF).

The effect of extra lesions on procedural outcome is unclear with studies suggesting there is reduction of AF recurrence. However, these studies relied heavily on 24-hour Holter recordings which have shown to have rather poor subclinical AF detection rates (5.5%) due to its intermittent nature. Furthermore, AF recurrence is considered as an ablation failure and AF burden reduction on the patients is not taken into consideration. Implantable cardiac monitors (ICMs) offer the advantage of continuous monitoring of the patient and offer high AF detection rates.

Objective

This study aims at evaluating the effect of extra lesions on the success rate of the procedure as well as on the AF burden change achieved on the patients.

Methods

This retrospective study included 33 patients (67% male; 57 ± 12 years; 26% Non-Paroxysmal AF) which were implanted with the Reveal LINQ, an ICM with AF detection rates of up to 96% that continuously classifies the heart rhythm of the patient analyzing its cardiac cycle and stores the daily AF burden in minutes/day. The ICM was implanted 134 ± 97 days before the ablation procedures, which were classified as PVI or PVI plus extra lesions, and the patients were followed up for 223 ± 111 days.

The patients were also divided into two classes: those with AF recurrence, defined as those with a detected episode outside the 3-months blanking period, and those without.

Results

Of the 33 patients analyzed, 21 had PVI only and 12 had PVI plus extra lesions. From those with PVI only, 15 (71%) had AF recurrence with a median burden reduction of 83% out of which 8 (53%) had a burden reduction > 80%. From the patients which had PVI plus extra lesions, 10 (83%) had recurrence with a median burden reduction of 84% out of which 6 (60%) had a burden reduction > 80%. 6 patients had a median burden increase of 222%, out of which 3 underwent PVI plus extra lesions (median burden increase of 360%) and 3 had PVI only (median burden increase 83%).

Figure 1 shows the AF burden detected in minutes/day for the patients with AF recurrence divided into pre ablation (PRE), blanking period (BP) and post ablation (POST). The markings show those patients that underwent PVI plus extra lesions (EL).

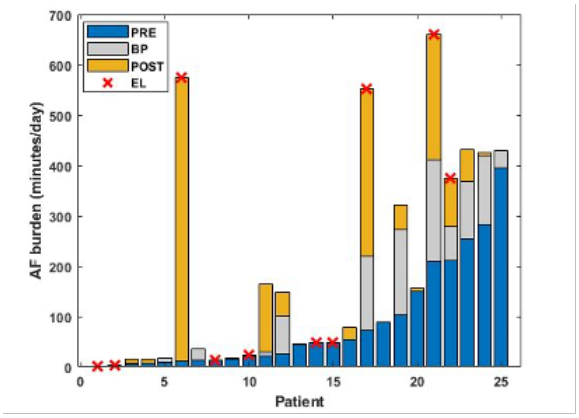

Figure 1: AF burden detected in patients with AF recurrence.

Discussion

Although a higher proportion of patients with PVI plus extra lesions had AF recurrence, a significant proportion of those with recurrence also had AF burden reduction > 80%. Moreover, for a small subgroup of patients in which the AF burden increased after CA, those with PVI plus extra lesions showed a higher increase in AF burden. This indicates that extra lesions could be indeed beneficial to some patients, especially in reducing the AF burden and, in doing so, increasing the quality of life of the patient.

Source Estimation in Cardiac Fibrotic Substrate from Intracardiac Signals

Pascual Tejero Cervera[1], Jorge Sánchez[2], Olaf Dössel[3], and Axel Loewe[2]

[1]Karlsruhe Institute of Technology, Institute of Biomedical Engineering, Karlsruhe, Germany
[2]Universistat Politècnica de València, Departamento de Ingeniería Electrónica, València, Spain

Background

Atrial fibrillation (AF) is a supraventricular tachyarrhythmia characterized by an uncoordinated rhythm of the atria. Often, fibrosis, which is the appearance of interstitial myofibroblasts and collagen, is associated with recurrent arrhythmia for AF. Ablation therapies can be an effective alternative to stop it, but it is necessary to explore a methodology that precisely localizes regions that sustain and promote AF.

Objective

Explore an inverse reconstruction by obtaining the signals from the electrograms of simulated reentrant activity in and around fibrotic patches. We obtain a map of the transmembrane voltages (TMV) of the cardiac tissue to localize strategic points in the cardiac tissue that promote AF.

Methods

Tissue patches of 50x50x1 mm with a spatial resolution of 0.2 mm were simulated in openCARP. Electrograms were computed with three different grids of electrodes (8x8, 12x12 or 16x16) with an interelectrode distance of 3 mm at two distinct distances to the tissue, 0.5 or 1 mm.

Simulations have been carried out so far in a control case (plane wave), reentry case and fibrotic tissue (plane wave with two different tissues of 10% and 60% collagen respectively, and both with 2% of myofibroblasts and the rest were myocytes).

Reconstruction of the transmembrane voltage at the tissue surface was performed in MATLAB software using a second order Tikhonov regularization, which deals with the ill-posedness of the inverse problem. Additionally, the Boundary Element Method was used to calculate the extracellular potentials of the sources at the surface of the tissue resembling unipolar electrograms.

The root mean square error (RMSE) of activation times (AT) was calculated to validate the methodology between the reconstructed signals (obtained in MATLAB) and the signals from the electrodes (ground truth from openCARP). ATs were calculated using the position at a time of the minimum value of the first derivative. Afterward, the minimum and maximum values of the AT were computed, and the RMSE was calculated between the ground truth and reconstruction with the same parameters (equal distance and electrode grid).

Results

Table 1 shows the RMSE of the maximum and minimum of AT between simulations with the same parameters. The RMSEs are lower for the control and reentry case (the latter with one exception) compared to the fibrotic case.

	Distance (mm)	Min and max RMSE (ms)		
		Electrode grid		
		8x8	12x12	16x16
Control case	0.5	(3,2)	(2,4)	(2,3)
	1	(5,2)	(3,4)	(4,8)
Reentry case	0.5	(3,2)	(12,4)	(12,8)
	1	(3,2)	(1,6)	(26,268)
Fibrotic case	0.5 (10% collagen)	(16,13)	(9,16)	(5,24)
	0.5 (60% collagen)	(74,25)	(0,38)	(0,38)

Table 1: RMSE of the minimum and maximum AT for the control case, reentry case and fibrotic case for each of the electrode distributions.

Discussion

In the control case, the propagation of the tissue is homogeneous; it is expected that the reconstruction will be similar to the ground truth and most errors obtained are not high. On the other hand, the good results in the reentry case determine that the methodology is also useful for the 8x8 and 12x12 electrodes. However, increasing the tissue electrode distance leads to an increase of the error, as it can be seen for the electrode grid of 16x16.

Finally, for the case of fibrotic tissue, higher error values were obtained. Although these errors could indeed be reduced by optimizing parameters (e.g., lambda value for the Tikhonov regularization), the values obtained are acceptable when the errors are lower than 20 ms.

To conclude, some reconstructions could improve and reduce the RMSE to precisely localize the reentry voltage points to stop AF effectively.

DGM is able to Distinguish between Dominant and Bystander Cycles in In-Silico and Clinical Double Loop Atrial Tachycardias

Enid Van Nieuwenhuyse[1], Lars Lowie[1], Sander Hendrickx[1], Jorge Sánchez[2], Sebastien Knecht[3], Mattias Duytschaever[3], Alexander V. Panfilov[1], and Nele Vandersickel[1]

[1]Deparment of Physics and Astronomy, Ghent University, Ghent, Belgium
[2]Institute of Biomedical Engineering, KIT, Karlsruhe, Germany
[3]AZ Sint-Jan Hospital Bruges, Bruges, Belgium

Background

Recently, Directed Graph Mapping (DGM) has shown to be able to automatically identify the reentry cycles and targets to ablate complex atrial tachycardias (ATs). However, sometimes, DGM found an additional reentry circuit which was not confirmed with entrainment maneuvres (EM) as a dominant reentry but as a bystander reentry.

Objective

We aimed to optimize the DGM software and add new features to automatically distinguish between the dominant and bystander cycle in clinical ATs with the aid of in-silico simulations. The simulations were based on a clinical case of AT and were used to test and experiment with the physiological and dynamical conditions of the double loop.

Methods

We made use of an accurate model of the left atrium and openCARP (Figure 1 A) to induce an in-silico double loop. A localized reentry at the anterior wall around a scar and a mitral valve reentry were initiated and depending on the size of the scar tissue (Figure 1 B), the mitral reentry shifted from a bystander to equally dominant with respect to the localized reentry. In-silico EMs were performed to test the behavior of each reentry DL cycle (Figure 1 B).

Results

Upon increase of the length of the scar, the region of collision between the colliding wavefronts of the dominant and bystander cycle shifted from connectivity with the mitral valve to an intermediate position between the scar and the mitral valve. This region emerged in the directed graphs by visualization of the opposing arrows (called Region Of Collision or ROC) in DGM (Figure 1 B). This was then tested on 9 cases of complex double loop ATs (Figure 1 C (for 2 cases)).

Discussion

In 8/9 clinical cases of AT, DGM is able to distinguish between dominance in double loop ATs. The ROC is therefore a valuable addition to DGM.

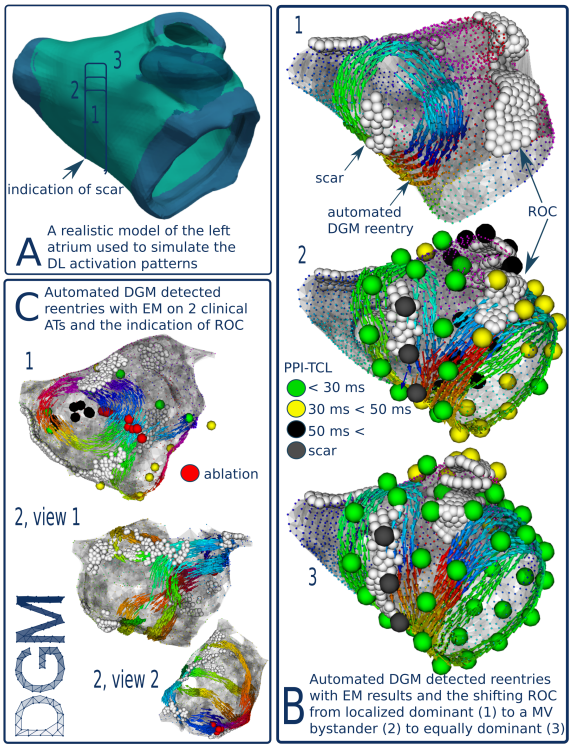

Figure 1: A. The in-silio LA setting with the indication of the scar regions for a shifting dominance. B. Application of the ROC on the in-silico AT cases with shifting dominance and C. for 2 clinical cases of AT.

Directed Network Mapping Hints the Ablation Strategy for Atrial Flutter: a Proof of Concept

Muhamed Vila[1], Massimo W. Rivolta[1], Giorgio Luongo[2], Axel Loewe[2], and Roberto Sassi[1]

[2]Dipartimento di Informatica, Università degli Studi di Milano, Milan, Italy
[2]Karlsruhe Institute of Technology, Institute of Biomedical Engineering, Karlsruhe, Germany

Background

Atrial flutter (AFL) is typically characterized by electrical activity propagating around specific anatomical regions and it is usually treated with catheter ablation. In this study, we modeled the electrical propagation pattern of AFL using directed network mapping (DNM). DNM is a recent method that makes use of network theory (NT) to characterize the electrical propagation [1, 2], such as the identification of cycles and focal points. The network is composed by nodes and edges resembling electrodes located across the atrial surface and the direction of the electrical propagation from one electrode to another.

Objective

The aim of the study was to verify whether DNM can recommend an ablation strategy to stop the mechanism generating AFL.

Methods

To test the algorithm, we set up a computational scenario based on a simulated AFL around the mitral valve in counterclockwise direction, as implemented in a previous work [3]. Electrograms and 3D anatomy were used in the DNM algorithm to build the network N. Then, electrical cycles were detected using a standard network search algorithm. In order to recommend ablation lines in an automatic fashion we proceeded as follows. First, a second network A, based on the Voronoi tessellation, was built on top of N in such a way that the edges connecting the nodes of A would cross the edges of N (thus resembling an ablation line capable of interrupting the electrical propagation between two connected electrodes). A list of all possible ablation lines from the network A was built using an implementation of the shortest path algorithm. Then, among these, we determined those capable, by themselves, of stopping the electrical cycles (and possibly the AFL).

Results

We identified all the ablation lines capable of interrupting, at the same time, every cycle detected in N. An example is in Figure 1.

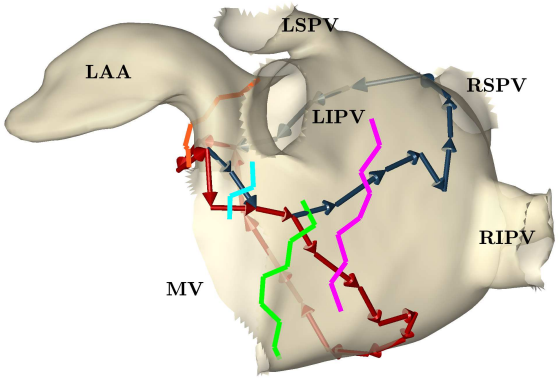

Figure 1: 3D model of the left atrium along with the detected cycles (red and blue arrows) and ablation lines (magenta, green, cyan and orange).

Discussion

We proposed a proof-of-concept algorithm, based on DNM, to automatically recommend ablation lines for the treatment of AFL.

References

[1] Vandersickel, N. et al., "Directed networks as a novel way to describe and analyze cardiac excitation: Directed graph mapping," *Front Physiol*, vol. 10, p. 1138, 2019.

[2] Vila, M. et al., "Directed network mapping approach to rotor localization in atrial fibrillation simulation," in *Conf Proc IEEE Eng Med Biol Soc*, 2021.

[3] Luongo, G. et al., "Non-invasive characterization of atrial flutter mechanisms using recurrence quantification analysis on the ECG: A computational study," *IEEE Trans Biomed Eng*, vol. 68, pp. 914–925, 1 2021.

The Extended ECG Improves Classification of Atrial Fibrillation Type and Prediction of Recurrence after Catheter Ablation

Stef Zeemering[1], Matthias Zink[1,2], Ben Hermans[1], Rita Laureanti[3], and Ulrich Schotten[1]

[1]Cardiovascular Research Institute Maastricht (CARIM), Physiology, Maastricht, the Netherlands
[2]University Hospital RWTH Aachen, Department of Internal Medicine 1-Cardiology, Aachen, Germany
[3]Politecnico di Milano, Department of Electronics, Information and Bioengineering, Milano, Italy

Background

The standard 10-second 12-lead electrocardiogram (ECG) is the default tool to diagnose ongoing atrial fibrillation (AF). Suboptimal lead placement to capture atrial conduction properties and short recording length may however limit its use as a tool to classify AF complexity and predict treatment outcome.

Objective

We investigated the added value of features derived from an extended ECG (eECG) with additional atrial-specific lead locations and longer recording length, when classifying AF type and predicting AF recurrence after catheter ablation, compared to features derived from the standard ECG.

Methods

ECGs with 3 additional atrial leads, 5-minute duration, and 500 Hz sampling frequency, were recorded in 242 patients before catheter ablation of AF, during sinus rhythm (SR, n=159) or AF (n=83). In SR features of the signal averaged P-wave (amplitude, area, entropy, and complexity) and beat-to-beat P-wave variability were computed. In AF F-wave features (dominant frequency, spectral organization index and entropy, amplitude, and variability) were determined. P- and F-wave features were used to classify AF type (paroxysmal or persistent AF) and to predict AF recurrence within 1 year after ablation. Classification and prediction models were constructed using feature selection (elastic net logistic regression) and performance (area under the receiver operation characteristics curve, AUC) was compared to models restricted to features that could be derived from a standard 10-second 12-lead ECG.

Results

Classification of paroxysmal/persistent AF using SR ECGs (n=119/40 respectively) was improved by using eECG P-wave features compared to standard features (median AUC 0.76 vs 0.58, $p < 0.001$, using P-wave amplitude, entropy, complexity, and variability), also after correcting for clinical characteristics. In AF ECGs a small improvement in classification of AF type (n=30/53) was observed when comparing standard and eECG models that corrected for clinical characteristics (AUC 0.74 vs 0.71, $p < 0.01$, using F-wave amplitude, variability, and weight). Follow-up of atrial rhythm after ablation was available in 161 patients (SR ECG: n=110, 32 AF recurrences; AF ECG: n=51, 31 recurrences). Prediction performance of recurrence after ablation was poor using standard P-wave features but improved by using eECG features (AUC 0.60 vs 0.70, $p < 0.001$, using P-wave entropy and complexity), and further increased when complemented by clinical characteristics (AUC 0.81, $p < 0.001$ compared to eECG model, using AF type). Both standard and eECG F-wave features prediction models performed well (AUC 0.75 vs 0.78, p=0.06, using dominant frequency and organization index). Performance increased by adding clinical characteristics (AUC 0.81 and 0.83, using history of vascular disease).

Discussion

P- and F-wave features of the extended ECG enable moderate to good classification of paroxysmal versus persistent AF and prediction of AF recurrence after catheter ablation. The extended ECG significantly improved classification or prediction performance with respect to a standard 10-second 12-lead ECG.